Application of the advanced adiabatic approach to charge exchange in slow collisions between H and O^{8+}

K. Richter*

Fakultät für Physik, Hermann-Herder-Strasse 3, 7800 Freiburg, Federal Republic of Germany

E. A. Solov'ev

Department of Theoretical Physics, St. Petersburg University, St. Petersburg, Russia

(Received 25 November 1992)

We study charge exchange in slow atomic collisions within the framework of the advanced adiabatic approach [Grozdanov and Solov'ev, Phys. Rev. A **42**, 2703 (1990)]. In this approach, nonadiabatic transitions near hidden or avoided crossings are related to branch points connecting adiabatic potential curves at complex values of the internuclear distance. A program package has been developed that automatically takes into account all relevant nonadiabatic transition amplitudes for the calculation of charge-transfer cross sections. The present method allows the inclusion of a large number of molecular-orbital basis functions and turns out to be extremely fast. As an example, partial and total cross sections are calculated for charge exchange in slow $O^{8+}+H(1s)$ collisions. The results are compared to previous theoretical and experimental data.

PACS number(s): 34.10.+x, 34.60.+z, 34.70.+e

I. INTRODUCTION

Charge transfer in slow atomic collisions between highly charged ions and hydrogen is of current interest in atomic and plasma physics because of its role in the energy balance and diagnostics of fusion and astrophysical plasmas. One important mechanism that leads to energy loss from the plasma is caused by impurity ions which capture electrons in their excited states and decay into lower states by emitting radiation. Therefore a great deal of theoretical and experimental effort has been made to determine the corresponding electron-capture cross sections (see, for example, the reviews by Janev and Winter [1], Gilbody [2], Fritsch and Lin [3], and Barat and Rocin [4]).

Experimentally, much progress has been made due to the development of modern sources for highly charged ions. Total electron-capture cross sections for C^{6+} and O^{8+} collisions with hydrogen have been measured, for example, by Dijkamp, Čirič, and de Heer [5] and Meyer *et al.* [6]. Additionally, photoemission spectroscopy of the excited highly stripped ions after charge exchange represents a powerful technique to yield information of partial cross sections for electron transfer into individual (n,l) subshells of the projectile [7].

Several theoretical investigations have been performed to describe slow collisions of highly stripped ions with hydrogen. Fritsch and Lin [8], for example, expanded the time-dependent electronic wave function in an extended basis set of atomic orbitals and solved the corresponding close-coupling equations. Green, Shipsey, and Browne (in the case of $C^{6+}H$ [9]) and Shipsey, Green, and Browne (for $O^{8+}H$ [10]) used large basis sets of traveling molecular orbitals. Olson applied the classical trajectory Monte Carlo method to ion-atom collisions [11]. The role of rotational coupling for the cross sections had previously

been pointed out by Vaaben and Briggs [12].

The usual close-coupling calculations require information about the adiabatic potential curves and nonadiabatic coupling matrix elements for *real* values of R. In the present work we report on an alternative method to calculate cross sections of slow collisions, i.e., the advanced adiabatic approach. Within this framework nonadiabatic transitions (due to radial couplings) are approximated by transition amplitudes in the vicinity of avoided or so-called *hidden* crossings of the adiabatic potential curves. The corresponding probabilities for nonadiabatic transitions are determined by calculating contour integrals in the *complex* R plane enclosing the branch points, which are related to avoided crossings. In addition rotational couplings are included. In this approach the probability for an inelastic transition as a result of the collision process is decomposed into a sequence of transition amplitudes of individual nonadiabatic transitions. Each partial cross section for the electron capture into a final (n,l) subshell of the projectile is determined by the sum over all possible paths that connect the initial adiabatic state with the final adiabatic molecular orbital (via hidden and avoided crossings and rotational couplings).

In a recent work [15] this method has been applied to slow $He^{2+}H$ collisions, taking into account only the dominant nonadiabatic transitions. A program package has now been developed that automatically searches for all (relevant) branch points connecting adiabatic potential curves and calculates the corresponding probabilities for the entire set of nonadiabatic transitions. Finally, the resulting S matrix, which is defined as a product of elementary S matrices for the individual transitions induced by the separated branch points, is integrated over the impact parameter. Thus we simultaneously obtain partial cross sections for arbitrary initial and final states in a given molecular-orbital basis set. This program package

is designed for use as a black-box routine which only re-
quires the charges of the nuclei and the basis size as input
parameters. To give an estimate of the speed, the pro-
gram takes about 20 minutes on a PC/AT to calculate
all cross sections for the collision process mentioned be-
low, including all states up to the united-atom principal
quantum number $n = 10$, i.e., 220 molecular orbitals.

In the present work we will apply the advanced adia-
batic method to the slow collision process of the type

$$O^{8+} + H(1s) \to O^{7+}(nl) + H^+. \tag{1}$$
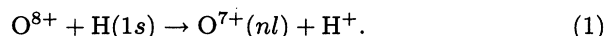
Total cross sections, partial cross sections for electron
capture into O^{7+} n shells and individual (n, l)-subshell
occupation probabilities are calculated. Collisions in-
cluding O^{8+} as well as C^{6+} ions are of particular impor-
tance for energy loss from fusion plasmas (for detailed in-
formation on these collision processes we refer the reader
to Ref. [13]).

In Sec. II we will summarize the main features of the
advanced adiabatic theory and describe our method to
calculate cross sections. The results for total as well as for
partial (n, l) cross sections are discussed and compared
to other calculations in Sec. III.

II. THEORY AND METHOD

A. The adiabatic approach

In the following we will briefly describe the main fea-
tures of the underlying theory of nonadiabatic transi-
tions, which is explained in detail in Refs. [14, 15]. We
assume classical uniform straight-line motion of the nu-
clei during the collision process. $\mathbf{R} = (vt, \rho)$ is the inter-
nuclear distance within the scattering plane (X, Y). The
relative nuclear velocity along the X axis is denoted by
v (= const) and ρ is the impact parameter.

As a first step we solve the stationary Schrödinger
equation for the electron in the Coulomb fields of two
fixed nuclei with charges Z_1, Z_2 and distance R (atomic
units are used throughout this work):

$$\left[-\frac{1}{2}\Delta_\mathbf{r} - \frac{Z_1}{|\mathbf{r} + \mathbf{R}/2|} - \frac{Z_2}{|\mathbf{r} - \mathbf{R}/2|} \right] \phi(\mathbf{r}, R)$$
$$= E(R)\phi(\mathbf{r}, R). \tag{2}$$

$\mathbf{r}$ denotes the distance from the electron to the midpoint
of the internuclear line. As is well known, the Schrödinger
equation (2) is separable in prolate spheroidal coordi-
nates

$$\lambda = \frac{r_1 + r_2}{R}, \quad \mu = \frac{r_1 - r_2}{R}, \tag{3}$$

and the azimuthal angle φ with respect to the inter-
nuclear axis. r_1 and r_2 are the distances between the
electron and the nuclei. The solution of the Schrödinger
equation (2) takes the product form

$$\phi(\mathbf{r}, R) = F_{n_\lambda}(\lambda)G_{n_\mu}(\mu) \exp(im\varphi), \tag{4}$$

where $F_{n_\lambda}(\lambda)$ and $G_{n_\mu}(\mu)$ are solutions of the separated
quasiradial (λ) and quasiangular (μ) differential equa-
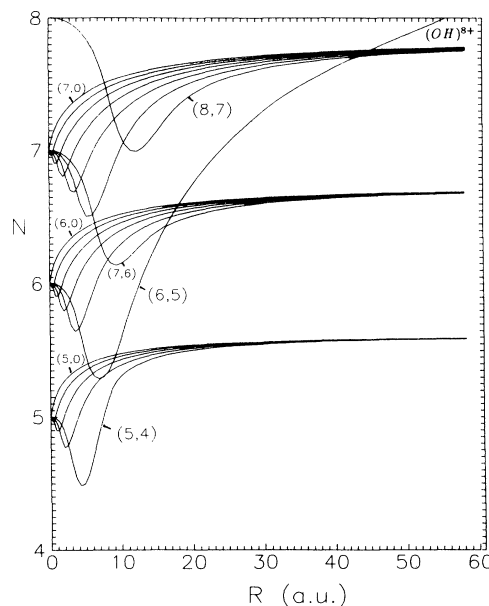tions, respectively. We use the method of continued frac-

FIG. 1. Part of the correlation diagram for $(OH)^{8+}$. The
effective quantum number $N = \sqrt{-(Z_1 + Z_2)/2E}$ is plotted
as a function of the internuclear distance R. Selected energy
curves are labeled by their united-atom quantum numbers
(n, l). For clarity only states with $m = 0$ are shown. The ini-
tial state $O^{8+}+H(1s)$ is indicated at the right-hand edge of the
diagram. The degenerated manifolds in the separated-atom
limit describe states $O^{7+}+H^+$ with O^{7+} principal quantum
numbers $n' = 5, 6, 7$.

tions [16] to generate exact energy potential surfaces in
the *complex* R plane. The energy curves for real val-
ues of R are just the usual Born-Oppenheimer potential
curves. Figure 1 depicts selected energy curves which we
have calculated for the system $(OH)^{8+}$ for real R. The
corresponding molecular-orbital (MO) states are com-
pletely characterized by the azimuthal quantum num-
ber m of the electronic angular momentum projected
onto the internuclear axis and the MO quantum num-
bers n_λ, n_μ which label the number of elliptical and hy-
perbolical nodal surfaces of the wave functions, respec-
tively. There is a one-to-one correspondence between
the molecular set of quantum numbers (n_λ, n_μ, m) and
the spherical quantum numbers (n, l, m) of the united-
atom limit $(R \to 0)$, which are commonly used to clas-
sify adiabatic potential curves. The following relations
hold: $n = n_\lambda + n_\mu + |m| + 1$, $l = n_\mu + |m|$. In the
separated-atom limit $(R \to \infty)$, the MO quantum num-
bers n_λ, n_μ, m are linked to the parabolic quantum num-
bers (n_1, n_2, m) [15].

B. Nonadiabatic transitions at avoided
or hidden crossings

In slow atomic collisions, transitions between adiabatic
states occur in the vicinity of avoided crossings or hid-
den crossings of the energy potential curves. An avoided
crossing of two potential curves $E_1(R)$ and $E_2(R)$ at

real R reflects their exact crossing (the branch point) at a complex internuclear distance $R = R_c$ [15]. Transition matrix elements between two adiabatic states exhibit a singularity at the common complex branch point R_c, which causes a peak in the nonadiabatic coupling matrix element for $R \approx \mathrm{Re}(R_c)$ and intense transitions in the region of the avoided crossing. The transition probability due to the branch point is given by [19]

$$P = \exp\left(-\frac{2}{v}\Delta\right). \tag{5}$$

The generalized Massey parameter Δ is defined as an integral in the complex t plane

$$\Delta = \mathrm{Im} \int_{\mathrm{Re}[t(R_c)]}^{t(R_c)} \{E_1[R(t)] - E_2[R(t)]\}\, d(vt), \tag{6}$$

where $t(R)$ is the inverse function obtained from the classical trajectory $R = R(t)$ describing the relative nuclear motion. Using the straight-line approximation

$$R(t) = \sqrt{\rho^2 + v^2 t^2}, \tag{7}$$

the Massey parameter does not depend on the internuclear velocity v and takes the form

$$\Delta(\rho) = \mathrm{Im} \int_{\mathrm{Re}(R_c)}^{R_c} [E_1(R) - E_2(R)]\frac{dR}{\sqrt{1 - \rho^2/R^2}}. \tag{8}$$

The integral is to be taken along a straight line in the complex R plane, which connects the real axis with the branch point R_c. The expression (5) for the transition probability together with the Massey parameter in the form of Eq. (8) can alternatively be derived from the semiclassical expression

$$P(E, \rho) = \exp\{-2\,\mathrm{Im}[S(E, \rho)]\} \tag{9}$$

for the transition probability. $S(E, \rho)$ is the (action) integral

$$S(E, \rho) = \int_{\mathrm{Re}(R_c)}^{R_c} \{ \sqrt{2M[E - U(R, \rho) - E_1(R)]}$$
$$- \sqrt{2M[E - U(R, \rho) - E_2(R)]}\}\, dR. \tag{10}$$

E is the total energy, M is the reduced mass of the two nuclei, and

$$U(R) = \frac{Z_1 Z_2}{R} + \frac{L(L+1)}{2MR^2} \tag{11}$$

is the nuclear part of the effective potential. Expansion of the square roots in Eq. (10) for $E - U \gg E_1, E_2$ yields the expression (8) for the Massey parameter. The transition probability in Eq. (5) together with the Massey parameter (8) is asymptotically exact for small velocity v.

An advantage of the adiabatic approach is the explicit expression for the probability for each individual nonadiabatic transition. In the past a wider application of this

approach has been limited due to an insufficient knowledge of *all* existing avoided crossings between adiabatic energy curves. The analysis of the analytic structure of the potential curves in the complex R plane enabled the discovery of new series of branch points which are related to *hidden* crossings [14]. They do not manifest themselves in the pattern of the potential curves for real R; i.e., the potential curves do not explicitly show avoided crossings. Nevertheless the corresponding adiabatic states are coupled and the common branch points help to explain not only bound-bound transitions but also ionization processes [15]. Due to the present development of an efficient program code for the systematic determination of all significant branch points and the related transition probabilities [according to Eq. (8)], it is possible to study charge exchange via hidden and avoided crossings in a rigorous and effective manner.

In the following we will give a short classification of the different types of avoided crossings, since they play a key role in this approach [18]. The character as well as the existence of series of hidden or avoided crossings depends on the ratio Z_1/Z_2 of the charges. For charges as in the case of the $(OH)^{8+}$ system we can distinguish the following different types of transitions (see Fig. 1):

(i) For large internuclear distances, small isolated avoided crossings appear between the potential curves of adiabatic states located at different nuclei and characterized asymptotically by their parabolic quantum numbers (n_1, n_2, m) at center Z_1 and (n'_1, n'_2, m) at center Z_2. See, for instance, the quasicrossing of the potential curve of the initial channel $O^{8+}+H(1s)$ with the $(n = 8)$ manifold in Fig. 1. The corresponding Massey parameter, which is in general small, can be obtained within the Landau-Zener-approximation [17]:

$$\Delta = \pi \frac{(\Delta E_{\min})^2}{4\Delta F}. \tag{12}$$

In Eq. (12), ΔF denotes the slope difference of the corresponding diabatic potential curves and $\Delta E_{\min}$ the energy separation at the quasicrossing. These avoided crossings have been well known for a long time [17]. Since Δ is small, the system usually passes diabatically through the crossing, i.e., the character of the wave function remains conserved.

(ii) In the intermediate range of internuclear distances, series of branch points appear at values of the real part of R, where the region of classically allowed electronic motion switches from the two-center atomic geometry, exhibiting separated electronic motion in the vicinity of one nucleus, to the quasimolecular arrangement where the electron moves inside the common shared potential well of the two Coulombic centers. In this R region the electronic wave function changes from quasiatomic to molecular character. Each of the related so-called Q series [14] of branch points or hidden crossings connects an original potential curve (n, l, m) consecutively with all higher potential curves $(n + i, l + i, m)$. Therefore the quasiradial quantum number $n_\lambda = n - l - 1$ remains unchanged under the corresponding transitions. Within each Q series the imaginary parts of the branch points
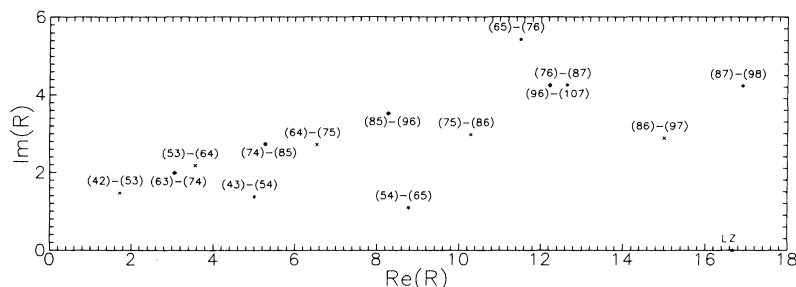
FIG. 2.   Positions of selected Q-series branch points in the complex R plane. The branch points connect MO states with $m = 0$, which are displayed in Fig. 1. (n,l)–$(n+1,l+1)$ denotes the corresponding nonadiabatic transition. The branch points near the real axis give rise to the dominant transitions. LZ labels the Landau-Zener branch point.

R_i, which connect MO states (n,l,m) and $(n+i,l+i,m)$, increase with increasing i. Thus, according to Eqs. (5) and (8), the dominant transition process is governed by the first branch point of each series connecting the MO states (n,l,m) and $(n+1,l+1,m)$. Therefore we will only consider here these branch points in our calculations. Calculations of the transition amplitudes of the higher branch points $(i > 1)$ yielded contributions of the order of a few percent and less. They are neglected in the following.

Figure 2 depicts the positions of the relevant Q-series branch points in the complex R plane which couple the adiabatic potential curves shown in Fig. 1. Roughly, strong transitions are related to branch points near the real axis. Thus the transition between the initial $[O^{8+}H(1s)]$ state, which correlates diabatically to the $(6,5,0)$ state (after passing the first two Landau-Zener crossings), and the MO state $(5,4,0)$ will be of particular importance for the capture process (see Sec. III).

(iii) Another group of branch-point series, the so-called S series, especially occurs at small internuclear distances. These series of hidden crossings appear at values of R where the electronic wave functions qualitatively change due to a passage from the quasimolecular two-center potential geometry at intermediate R to the "single-center," "united-atom" case. Each S_{lm} series consists of an infinite set of branch points $R_{lm}^{(n)}$ connecting pairs of MO potential curves (n,l,m) and $(n+1,l,m)$ consecutively for all $n \geq l+1$. All branch points of a given S_{lm} series are located within a small area of the complex R plane and converge to a common limit $R_{lm}^{(\infty)}$ [14]. The potential curves in Fig. 1, for example, have common S-series branch points at internuclear distances between $R = 0.12$ a.u. for $l = 1, m = 0$ and $R = 5.9$ a.u. for $l = 6, m = 0$.

The S series, as well as the Q series, of hidden crossings occur in regions of the internuclear distance whenever the adiabatic states can be associated (in the semiclassical limit) with unstable classical periodic orbits of the electron [22]. The instability of the related classical motion reflects the strongly enlarged transition probabilities between corresponding quantum MO states.

C. Treatment of rotational couplings

Due to the rotational symmetry of the system with regard to the internuclear axis, potential curves with dif-

ferent values of m cannot have common branch points, i.e., exhibit no radial coupling but only rotational coupling. For a complete description of the collision dynamics, rotational coupling between MO states of different azimuthal quantum number m must be included, too. For the present calculations rotational couplings have been calculated within the framework of the so-called *dynamical adiabatic approach* [15, 20]. This method had been developed with the aim of constructing modified adiabatic wave functions that are compatible with the physical boundary conditions in the limit $R \rightarrow \infty$. (The standard adiabatic wave functions for fixed nuclei do not contain Galilei translational factors, which arise from the motion of the nuclei, and therefore are incompatible with the large-R physical boundary conditions.) The idea of the dynamical adiabatic method, which is described in detail in Refs. [15, 20] can be summarized as follows: To solve the problem of momentum transfer a nonstationary scaling of the length is introduced by definition of a new independent variable

$$\mathbf{q} = \frac{\mathbf{r}}{R(t)}. \tag{13}$$

After an additional time transformation it was possible to transfer the original time-dependent Schrödinger equation (with moving Coulomb centers) into a new modified Schrödinger equation with the Coulomb centers staying at rest, i.e., there occurs no momentum transfer and the new dynamical adiabatic wave functions exhibit the correct boundary conditions. The price to pay for these improvements is the appearance of a velocity-dependent (perturbative) potential in the resulting Hamiltonian of the form

$$V(\omega) = \omega l_3 + \tfrac{1}{2}\omega^2 q^2, \quad \omega = \rho v \tag{14}$$

in addition to the two-center Coulomb potential. l_3 is the projection of the electronic angular momentum onto the direction perpendicular to the scattering plane. The "paramagnetic" part ωl_3 destroys the separability of the original two-center Hamiltonian. We are considering rotational couplings in the O^{8+}-H collisions as follows: For sufficient small velocity v we treat $V(\omega)$ as a perturbation that mixes the standard MO states of the pure two-center Coulomb problem, which are correct eigenstates for $v = 0$. The dominant contribution to the rotational couplings between standard molecular orbitals arises at

the united- and separated-atom limits, where the nearly degenerated MO states are shifted and strongly mixed due to the perturbation $V(\omega)$. Therefore we approximate the overall rotational coupling by using a perturbative treatment of the rotational couplings at small and large internuclear distance.

For partial cross sections the rotational coupling at large R is of crucial importance. We calculate rotational couplings at large R with the help of dynamical adiabatic basis states in second-order perturbation theory with respect to ω. The calculations represent the first application of the theoretical method, which can be found in Ref. [20].

The significance of rotational couplings at small internuclear distances for ion-atom collisions is well known, too [24]. At small R we numerically solve a system of close-coupling equations as had been done in Ref. [23].

D. Validity of the adiabatic approach

In our calculations we generally use the straight-line approximation for the motion of the nuclei. In the united-atom region the Coulomb motion of the nuclei is of considerable influence and we take it into account in the calculation of the rotational transitions. However, even in the united-atom region the difference in the calculations assuming straight-line and Coulombic motions of the nuclei is only of the order of a few percent.

The dynamical adiabatic approach represents a rigorous mathematical basis for a prescription of the asymptotic character of the results based on the standard MO states. In using the standard molecular orbitals for the calculation of transition probabilities [Eq. (5)] at hidden crossings, and the related Massey parameter [Eq. (8)], we neglect the additional potential $V(\omega)$. Thus the results are only exact in the asymptotic limit $v \to 0$, since $V(\omega)$ vanishes in this limit. However, it is easy to show [20] that the following relation holds between the Massey parameter $\Delta^{(0)}$ in the standard MO basis and the Massey parameter Δ in the dynamical adiabatic basis:

$$\Delta = \Delta^{(0)} + v^2 \Delta^{(1)} + O(v^3).\qquad(15)$$

Thus the transition probabilities [Eq. (5)] we use for the calculations are accurate up to the leading order in v.

The question of the validity of the adiabatic approach arises at sufficiently high collision velocities, when the transitions caused by hidden or avoided crossings become significant. Since the adiabatic approach is based on an asymptotic expansion, there do not exist any rigorous criteria for the range of validity. As a rule of thumb, the adiabatic assumption is justified up to velocities v where the cross sections approach their maxima.

E. Calculation of cross sections

Our procedure to obtain partial and total cross sections for slow atomic collisions is the following: In a first step all branch points are automatically determined and the related transition probabilities that depend on the impact parameter are calculated using the method presented above. Taking into account the additional ro-

tational couplings, the advanced adiabatic approach includes all types of nonadiabatic transitions.

We define an S matrix [21] whose elements S_{ij} denote the probability for an inelastic transition from the initial MO state $\{i\}$ to the final state $\{j\}$ after the collision. Each adiabatic state (n, l, m) can be labeled by an index i defined as

$$i = \tfrac{1}{6}(n-1)n(n+1) + \tfrac{1}{2}l(l+1) + m + 1.\qquad(16)$$

Starting with the initial S matrix $S_{ij}^{(0)} = \delta_{ij}$, the nth individual transition between two states $\{k\}$ and $\{l\}$ induced by a branch point at internuclear distance R_n yields a change in the S matrix, i.e., $S^{(n)} = \hat{V}_{kl} S^{(n-1)}$. If P_{kl} denotes the probability for a transition between state $\{k\}$ and $\{l\}$, the kth and lth column of the S matrix changes according to

$$S_{ik}^{(n)} = S_{ik}^{(n-1)}(1 - P_{kl}) + S_{il}^{(n-1)} P_{kl},$$

$$\qquad(17)$$

$$S_{il}^{(n)} = S_{il}^{(n-1)}(1 - P_{kl}) + S_{ik}^{(n-1)} P_{kl}.$$

The final S matrix is the result of all successive individual transitions between adiabatic states. After integration of the S matrix over the impact parameter, we finally obtain a complete set of cross sections $\sigma_{ij}(v)$ between arbitrary initial and final states in a given MO basis.

We should point out that quantum interference effects between different possible paths along adiabatic potential curves which reach the same final state are not included in the construction of the transition matrix. Such interference effects are crucially important for differential cross sections with fixed impact parameter. The contribution from interference effects has the form $\cos(-2\phi/v) = [1 + \cos(2\phi/v)]/2$, where ϕ is the phase shift. After integration over the impact parameter, the contribution of the second (interference) term
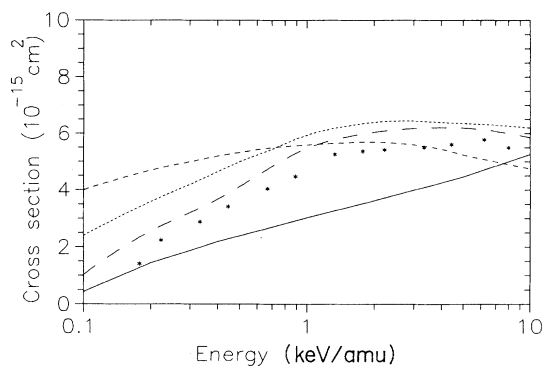

FIG. 3. Total cross sections for electron transfer in O^{8+}H collisions. Present advanced adiabatic approach (solid line); atomic-orbital expansion calculation by Fritsch and Lin [8] (long dashes); MO calculation by Shipsey, Green, and Browne [10] (dotted line); multichannel Landau-Zener calculation with rotational coupling by Janev, Belic, and Brandsen [25] (short dashes). Experimental results from Meyer et al. [6] (asterisks).

appears only in second order with respect to the small asymptotic velocity parameter v. Thus corrections due to interference effects are beyond the accuracy range of the asymptotic adiabatic theory used in the present work and of the same order in v as other contributions of the full Hamiltonian which are ignored within an adiabatic approach.

In our cross-section calculations for collisions between bare oxygen and hydrogen, we use a basis set of all MO states with united-atom quantum number $n < 11$, i.e., 220 states. In this case we take into account 146 branch points and simultaneously obtain cross sections for $220 \times 221/2 = 24\,310$ inelastic channels connecting all initial and final states. From the large amount of data we extract only the cross sections that are relevant for charge-transfer processes from H($1s$).

III. RESULTS: APPLICATION TO O^{8+}+H($1s$) COLLISIONS

Figure 1 depicts a part of the MO correlation diagram for the (OH)$^{8+}$ collision system. Only molecular orbitals with $m = 0$ are displayed. The initial configuration with the electron in the hydrogenic $1s$ state correlates to the
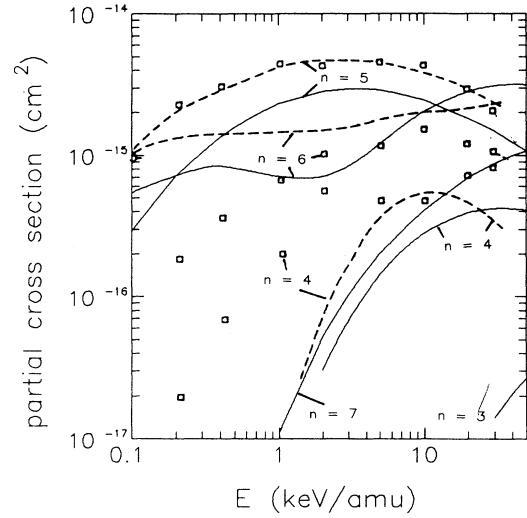

FIG. 4. Partial cross sections for electron transfer into $n = 3, 4, 5, 6, 7$ orbitals of O^{7+}, adapted from Fig. 10 of Ref. [8]. The present results are indicated by solid lines; data from atomic-orbital expansion calculations by Fritsch and Lin [8] are indicated by open squares and results from MO calculations by Shipsey, Green, and Browne [10] by dashed lines.

TABLE I.   Cross sections (in 10^{-17} cm^2) for electron transfer in O^{8+}+H($1s$) collisions into n shells (σ_n) and (n, l) subshells (p_{nl}) of O^{7+}. σ_{tot} denotes the total electron-capture cross section. Cross sections lower than 10^{-19} cm^2 have been omitted.

| E (keV/amu)	n	σ_{tot}	σ_n	p_{n0}	p_{n1}	p_{n2}	p_{n3}	p_{n4}	p_{n5}	p_{n6}	p_{n7}
0.1	5	44.2	31.2	4.4	10.3	9.9	5.2	1.2			
	6		13.0		1.5	4.1	4.5	2.4	0.5		
0.2	5	120.9	75.7	7.0	19.2	24.5	18.4	6.4			
	6		45.1	0.2	1.4	4.8	9.3	14.7	14.5		
0.4	5	218.9	134.7	8.9	28.1	42.5	37.4	17.9			
	6		84.2	0.6	3.1	8.1	14.8	23.6	34.1		
1.0	4	304.0	0.5	0.1	0.2	0.2	0.1				
	5		231.5	9.5	35.8	68.5	76.0	41.7			
	6		70.9	1.0	3.3	7.1	13.1	19.9	26.5		
	7		1.1			0.1	0.1	0.2	0.3	0.3	
2.0	4	362.6	3.0	0.2	0.8	1.2	0.8				
	5		283.3	9.5	38.7	80.9	97.3	56.9			
	6		70.7	1.2	4.4	9.2	15.3	19.5	21.2		
	7		5.2	0.1	0.3	0.5	0.7	1.0	1.2	1.5	
	8		0.4					0.1	0.1	0.1	0.1
5.0	4	446.3	14.3	0.9	3.4	5.7	4.3				
	5		288.7	8.9	37.5	81.1	100.6	60.7			
	6		120.1	2.1	8.7	20.5	32.9	33.9	22.1		
	7		20.0	0.3	1.1	1.9	2.8	3.7	4.6	5.5	
	8		3.2	0.1	0.2	0.3	0.4	0.5	0.6	0.6	0.7
10.0	3	526.4	0.1		0.1	0.1					
	4		28.1	1.7	6.6	11.3	8.5				
	5		244.8	7.5	31.6	68.6	85.3	51.8			
	6		203.4	3.4	14.9	36.9	59.5	58.5	30.2		
	7		40.6	0.7	2.1	4.0	6.3	8.2	9.1	10.2	
	8		9.6	0.2	0.4	0.7	1.1	1.5	1.8	1.9	2.0
20.0	3	597.4	0.7	0.1	0.3	0.3					
	4		39.2	2.3	9.1	15.9	11.9				
	5		183.4	5.6	23.7	51.5	64.0	38.7			
	6		283.8	4.5	20.7	52.4	85.2	82.4	38.6		
	7		69.5	1.0	3.4	7.0	11.9	15.4	15.5	15.3	
	8		20.8	0.3	0.8	1.5	2.5	3.5	4.1	4.1	3.9
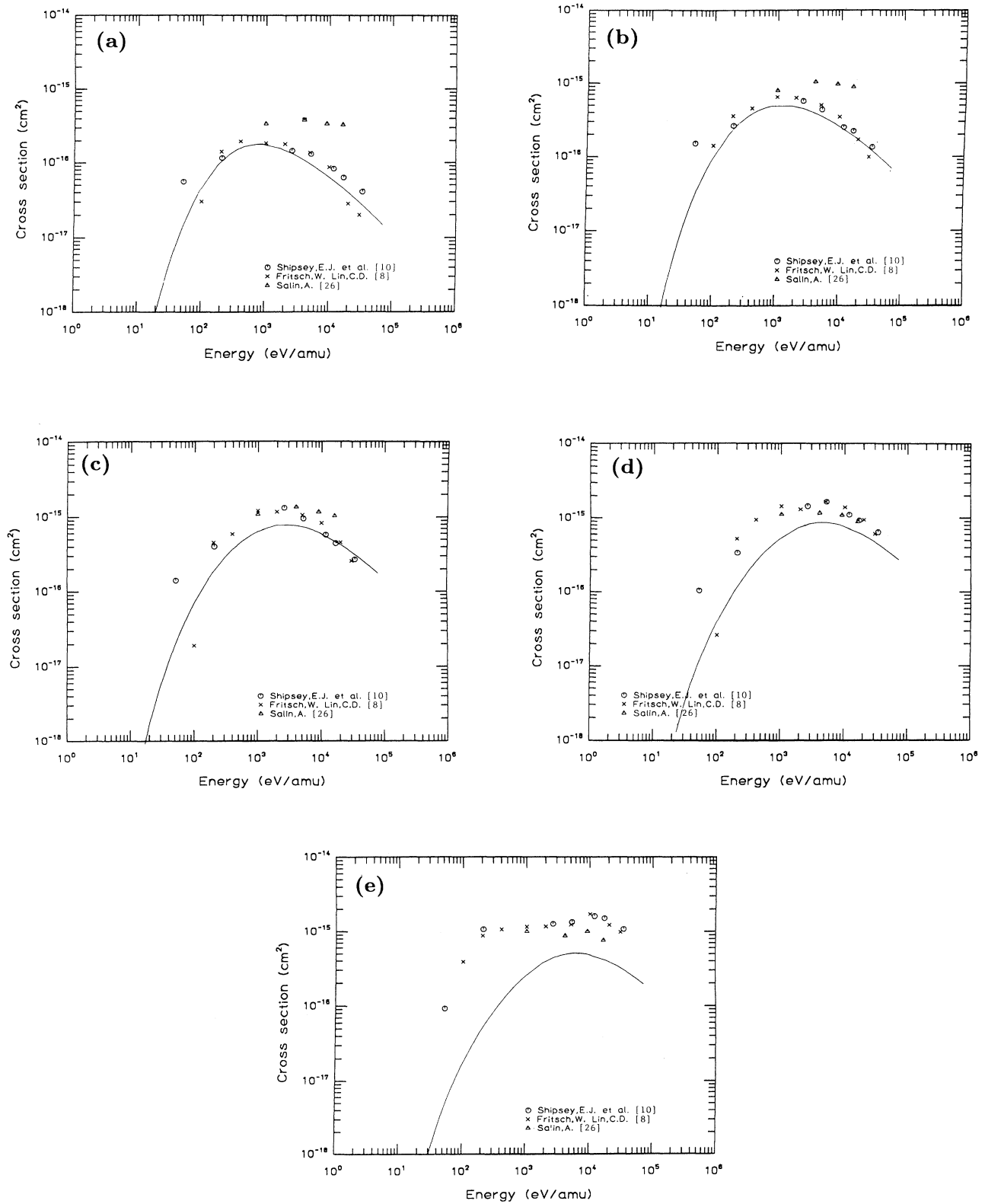
FIG. 5. Partial cross sections for electron transfer into individual $(n = 5, l)$ subshells of O^{7+}. Results for $l = 0, 1, 2, 3$, and 4 are depicted in parts (a), (b), (c), (d), and (e), respectively. Present results are indicated by solid lines. The other data are taken from Refs. [8, 10, 26].
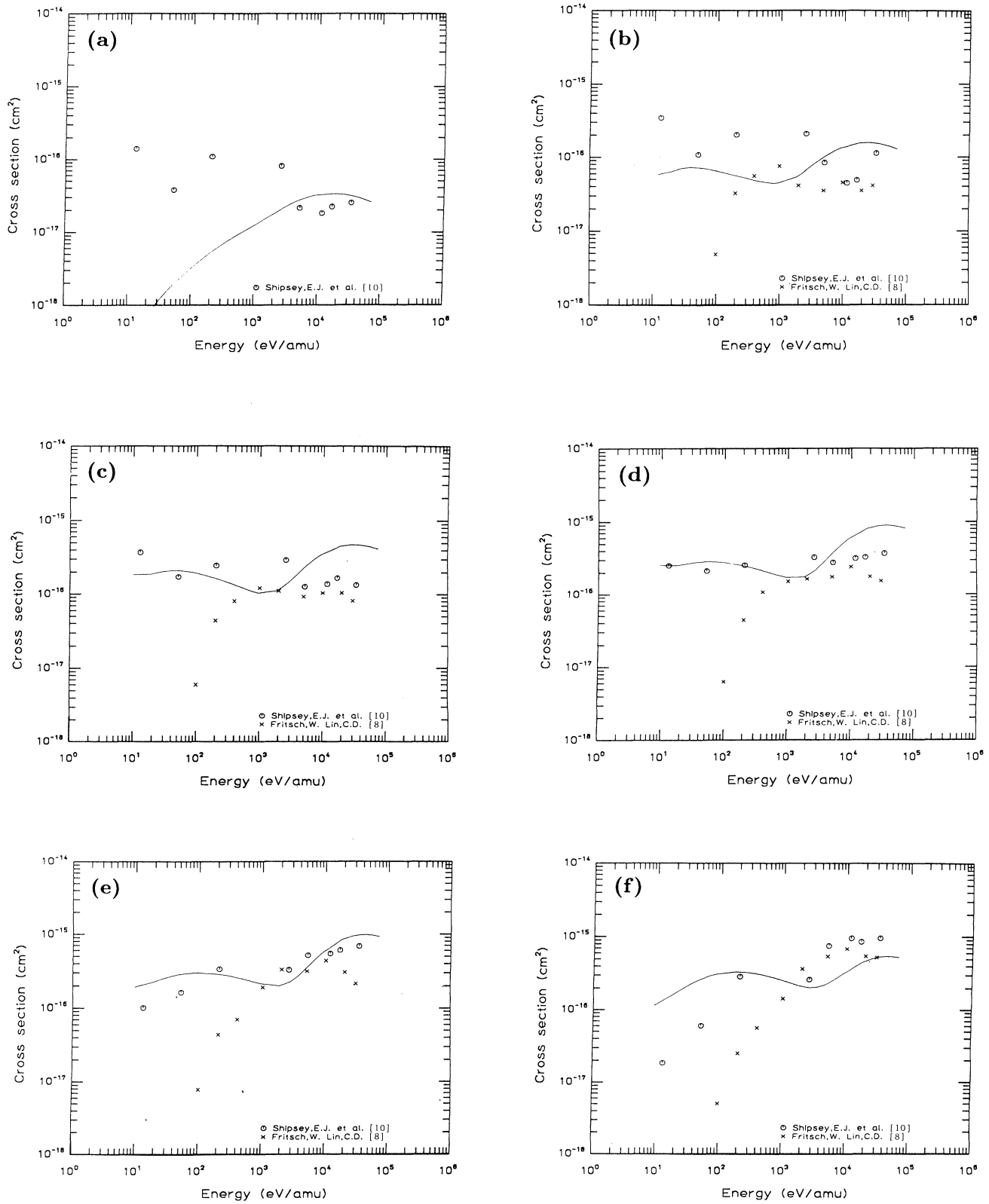
FIG. 6.   Partial cross sections for electron transfer into individual $(n = 6, l)$ subshells of O^{7+}. Results for $l = 0, 1, 2, 3, 4,$ and 5 are depicted in parts (a), (b), (c), (d), (e), and (f), respectively. Present results are indicated by solid lines. The other data are taken from Refs. [8, 10].

state (8,7,0) in united-atom classification. At low colli-
sion energies the initial state passes diabatically through
the first extremely small (8,7,0)–(7,6,0) avoided cross-
ing. The following (7,6,0)–(6,5,0) avoided crossing near
$R = 16.7$ a.u. then leads to dominant charge transfer
into the $(n = 6)$ shell of O^{7+}. At intermediate and
higher energies the initial state changes diabatically into
the (6,5,0) MO. In this case the (6,5,0)–(5,4,0) Q-series
avoided crossing near $R = 9$ a.u. mainly contributes
to dominant electron transfer into the O^{7+} $(n=5)$ shell.
Other (n, l) subshells are occupied under successive ra-
dial transitions governed by the Q series of branch points
discussed in Sec. II B. If the nuclei approach closer, radial
$(n, l, m) \rightarrow (n + 1, l, m)$ transitions arise due to S-series
branch points at small internuclear distances. They are
accompanied by rotational transitions between nearly de-
generated united-atom energy levels.

The main results of our calculations are summarized
in Table I, which contains total cross sections, par-
tial electron-transfer cross sections into O^{7+} n shells
$(n = 3, 4, 5, 6, 7)$, and specific cross sections for popu-
lation of individual (n, l) subshells. Our results for the
total cross sections are displayed in Fig. 3 (solid line)
in comparison with other theoretical and experimental
data from the literature. Electron-transfer mechanisms
in O^{8+}H collisions have been previously calculated by
Janev, Belic, and Brandsen [25], Salin [26], Shipsey,
Green, and Browne [10], Fritsch and Lin [8], and Harel
and Jouin [27]. Measurements have been performed by
Meyer et $al.$ [6]. As shown in Fig. 3, the cross sections
from the advanced adiabatic approach are in considerable
agreement with the experimental data at low collision en-
ergies, although they are significantly smaller than all the
other data in the intermediate-energy regime.

This difference can be traced back to the behavior of
the $n = 5$ partial cross sections. In Fig. 4 electron-
transfer cross sections into O^{7+} n shells from the present
calculations (solid lines) are compared with an MO study
from Shipsey, Green, and Browne [10] (open squares) and
close-coupling calculations of Fritsch and Lin [8] (dashed
lines) using an atomic-orbital basis set. Our data for the
electron capture into $n = 5$, which yield the dominant
contribution to the total cross section, lie systematically
below the results from the other calculations. Figure 4
also shows large discrepancies between $n = 4, 6, 7$ par-
tial cross sections obtained from the different approaches,
especially at low energies. In all there exists a certain
agreement between the present results and the data from
Fritsch and Lin, but large differences to the calculations
of Shipsey, Green, and Browne. As they noted [10], the
large $n = 6$ cross sections are mainly caused by (6,5,0)–
(6,5,1) rotational coupling.

The use of a large basis set of MO states allows us to
calculate electron transfer into higher n shells. As one

result the cross sections for $n = 7$ turn out to be larger
than the corresponding results for $n = 4$ (see Fig. 4).

Figures 5 and 6 give a detailed comparison between
the dominant transfer cross sections for individual (n, l)
subshells $(n = 5, 6)$ obtained by the present calculations
(solid curve) and previous investigations. The results
from our approach are in agreement with the other calcu-
lations at higher energies above the cross-section maxima
where the validity of our adiabatic approximation is not
ad hoc evident. Large discrepancies between the different
data mainly appear at small energies where the accuracy
of the adiabatic treatment should rise. In particular the
$n = 5$ cross sections exhibit differences in orders of mag-
nitude. The dip in the $n = 6$ cross sections of the present
work (see Fig. 6) appears due to an enhancement of the
cross section at low energies as a result of transitions at
the (7,6,0)–(6,5,0) avoided crossing at $R = 16.7$ a.u.

IV. CONCLUSION

The improved understanding of transition mechanisms
due to couplings between adiabatic potential curves at
hidden crossings (in addition to the visible avoided cross-
ings) has opened the possibility to take into account all
relevant couplings to study charge exchange and other
inelastic transitions in slow ion-atom collisions. In the
present work we have developed a systematical procedure
that allows for automatic calculations of cross sections as
the result of successive inelastic transitions at the com-
mon branch points of all MO potential curves involved.
The algorithm is fast and calculates simultaneously par-
tial cross sections for all initial and final states within a
given MO basis set. The method yields insight into the
physics of slow ion-atom collision processes since it is pos-
sible to examine the strength and influence of individual
nonadiabatic transitions between the MO states.

As an example we calculated total cross sections as
well as partial occupation rates for charge exchange into
(n, l) subshells of O^{7+} in slow O^{8+}+H($1s$) collisions. The
application of the method to collision processes of H with
other charged particles is straightforward [29].

A similar adiabatic method has recently been used [28]
to investigate an anomalous n dependence of electron
capture from atomic hydrogen by multicharged ions.

ACKNOWLEDGMENTS

* Present address: Université   Paris-Sud,   Institut de
  Physique Nucléaire, Division de Physique Théorique,
  91406 Orsay CEDEX, France.
[1] R. K. Janev and H. Winter, Phys. Rep. **117**, 265 (1985).

[2] H. B. Gilbody, Adv. At. Mol. Phys. **22**, 143 (1986).
[3] W. Fritsch and C. D. Lin, Phys. Rep. **202**, 1 (1991).
[4] M. Barat and P. Roncin, J. Phys. B **25**, 2205 (1992).
[5] D. Dijkamp, D. Čirič, and F. J. de Heer, Phys. Rev. Lett.

54, 1004 (1985).

[6] F. W. Meyer, A. M. Howald, C. C. Havener, and R. A. Phaneuf, Phys. Rev. A **32**, 3310 (1985).

[7] R Hoekstra, D. Čirič, F. J. de Heer, and R. Morgenstern, Phys. Lett. A **124**, 73 (1987); Phys. Scr. **T28**, 81 (1989).

[8] W. Fritsch and C. D. Lin, Phys. Rev. A **29**, 3039 (1984).

[9] T. A. Green, E. J. Shipsey, and J. C. Browne, Phys. Rev. A **25**, 1364 (1982).

[10] E. J. Shipsey, T. A. Green, and J. C. Browne, Phys. Rev. A **27**, 821 (1983).

[11] R. E. Olson, Phys. Rev. A **27**, 1871 (1983).

[12] J. Vaaben and J. S. Briggs, J. Phys. B **14**, L521 (1977).

[13] See contributed papers of the Proceedings on Carbon and Oxygen Data for Fusion Plasma Research, edited by R. K. Janev [Phys. Scr. **T28** (1989)].

[14] E. A. Solov'ev, Usp. Fiz. Nauk. **157**, 437 (1989) [Sov. Phys. Usp. **32**, 228 (1989)].

[15] T. P. Grozdanov and E. A. Solov'ev, Phys. Rev. A **42**, 2703 (1990).

[16] E. A. Solov'ev, Zh. Eksp. Teor. Fiz. **81**, 1681 (1981) [Sov. Phys. JETP **54**, 893 (1981)].

[17] L. D. Landau and E. M. Lifshitz, *Quantum Mechanics, Non Relativistic Theory* (Pergamon, New York, 1977).

[18] For a detailed description of the different types of (hidden) avoided crossings, see Refs. [14] and [15].

[19] E. C. G. Stueckelberg, Helv. Phys. Acta **5**, 369 (1932).

[20] T. P. Grozdanov and E. A. Solov'ev, Phys. Rev. A **44**, 5605 (1991).

[21] S is not the standard S matrix because its elements describe probabilities and not amplitudes.

[22] D. I. Abramov, S. Yu. Ovchinnikov, and E. A. Solov'ev, Phys. Rev. A **42**, 6366 (1990).

[23] T. P. Grozdanov and E. A. Solov'ev, J. Phys. B **15**, 3871 (1982).

[24] J. S. Briggs, Rep. Prog. Phys. **39**, 219 (1976).

[25] R. K. Janev, D. C. Belic, and B. H. Brandsen, Phys. Rev. A **28**, 1293 (1983).

[26] A. Salin, J. Phys. (Paris) **45**, 671 (1984).

[27] C. Harel and H. Jouin, J. Phys. B **21**, 859 (1988).

[28] J. Macek and S. Y. Ovchinnikov, Phys. Rev. Lett. **69**, 2357 (1992).

[29] R. Janev and E. A. Solovév (unpublished).